Received: 17 June 2019 | Revised: 5 September 2019 | Accepted: 10 September 2019

DOI: 10.1002/ese3.507

Energy Science & Engineering
Open Access

RESEARCH ARTICLE

Energy absorption from parks of point-absorbing wave energy converters in the Swedish exclusive economic zone

Jens Engström[1] | **Malin Göteman**[1] | **Mikael Eriksson**[1] | **Mikael Bergkvist**[1] | **Erik Nilsson**[2] | **Anna Rutgersson**[2] | **Erland Strömstedt**[1]

[1]Division of Electricity, Uppsala University, Uppsala, Sweden

[2]Department of Earth Sciences, Uppsala University, Uppsala, Sweden

Correspondence
Jens Engström, Division of Electricity, Uppsala University, Box 534, 75121 Uppsala, Sweden.
Email: jens.engstrom@angstrom.uu.se

Funding information
Swedish STandUP for energy research alliance; Energimyndigheten, Grant/Award Number: 42256-1

Abstract

In a future energy system based on renewable energy sources, wave energy will most likely play a role due to its high energy potential and low intermittency. The power production from parks of wave energy converters of point absorber type has been extensively studied. This is also the case for the wave energy resource at many coastal areas around the globe. Wave energy has not yet reached a commercial level, and a large variety of technologies exist; therefore, an established method to calculate the technical potential for wave energy has still not been established. To estimate the technical potential of wave energy conversion, some approximations inevitably need to be taken due to the systems high complexity. In this study, a detailed mapping of the wave climate and simulation of large arrays of hydrodynamically cross-coupled wave energy converters are combined to calculate the technical potential for wave energy conversion in the Swedish exclusive economic zone. A 16-year wave data set distributed in a 1.1 km × 1.1 km grid is used to calculate the absorbed energy from a park of 200 generic point absorbers. The areas with best potential have an average annual energy absorption of 16 GWh for the selected wave energy park adapted to 1 km^2 when using a constant damping, while the theoretical upper bound is 63 GWh for the same area.

KEYWORDS

point absorber, Swedish exclusive economic zone, technical potential, wave energy conversion, wave energy park

1 | INTRODUCTION

In the quest of replacing energy from fossil fuel by renewable energy, wave energy is one of the candidates. The theoretical global wave energy potential is estimated to be 32 PWh/y,[1] which is roughly twice the global energy use. The Atlantic coast in Europe is estimated to have an average resource of 290 GW out of which 32-48 GW is estimated to be technically achievable.[2] The most energetic sites in Europe are found outside Ireland and Scotland with average energy transports of 75 kW/m.[2] It is also worth noting that the average winter power level along the European Atlantic coast is twice as high as the average annual, coinciding with the energy demand pattern of the European society.[2]

To some extent, conclusions on the potential for wave energy conversion can be drawn from the wave climate. But a realistic technical potential also have to include areas like energy absorption of the wave energy converter (WEC),

electrical and mechanical energy losses. Thus, the technical potential for wave energy conversion can be formulated in many ways, with different levels of accuracy. The technical potential for wave energy conversion using point absorbers in Swedish waters has been studied previously,[3,4] where four locations with focus on the Baltic Sea were investigated and the wave energy conversion was represented by a constant capture width ratio and a utility factor. In that study, the annual energy delivered to grid from a 40 MW wave energy park located north of the island Gotland was calculated to 105 GWh. In another study,[5] the technical potential for the countries facing the North Sea was estimated using the wave climate and an average efficiency for wave energy conversion of 10%. A model for harvestable wave energy based on the offshore performance of full scale devices such as Pelamis and Wave Dragon were presented in.[6] They applied the model on the west coast of the Vancouver Island in Canada and calculated the harvestable wave energy up to 3000 MWh/y for a 750 kW Pelamis device.[6,7] The model used 5-year wave data in 3 hour intervals, and the result was calculated in four nautical minutes (7408 m) grid cells. The technical potential was calculated for three locations on the Atlantic coast of the Iberian Peninsula (Spain and Portugal) in,[1] where the optimal capture width as a function of wave energy period was calculated and combined it with a wave energy scatter diagram based on a 10-year data set to calculate a power matrix for a wave energy converter of point absorber type.

The global and regional wave climates have been extensively studied (see, eg,[1,8]). The wave climate off the Swedish west coast was investigated in detail at 13 locations in,[9] and the wave energy flux was found to have an average value of 5-6 kW/m in offshore locations. An overall study of the variations of the wave field in Swedish waters was presented in.[10] Using a spectral wave model in a 11 km × 11 km grid, the months with the highest waves were found to be November and December.

For large-scale utilization of wave energy from the oceans, it is required that a large number of WECs operate in unison. In particular, this is the case for a WEC concept based on point absorbers, which consists of large arrays of units with an individual spatial extent smaller than the wavelength of the incoming ocean waves. The complexity of modeling increases rapidly with the number of interacting WECs since the individual units interact by scattered and radiated waves. Thus, simulations tend to get very time-consuming when the number of interacting bodies grows. Assumptions can simplify the calculations and enable simulations of a large number of structures.[11,12] But the wave energy devices in focus here are separated by distances small enough for interaction effects to be significant.[13] Hydrodynamic interactions between the WECs are therefore included as far as possible in this paper.

Both the hydrodynamic and electrical interactions between devices in an array are important subjects. It can lead to a substantial increase or reduction in produced electric power for the array, depending on the geometry, interspacing between the devices and orientation relative to the wave direction.[14] On the other hand, the size of the wave energy park should be minimized to save costs on especially electrical cables and to minimize conflict with other interests in the coastal area. In addition, interconnecting wave energy converters in large wave power parks can reduce the fluctuations in power generation, which is beneficial for grid integration and this have been extensively studied.[15-17]

In this paper, we will combine detailed mapping of the wave climate and simulation of large arrays of hydrodynamically cross-coupled wave energy converters. We will use a 16-year wave data set distributed in a 1.1 km × 1.1 km grid of the Swedish exclusive economic zone (SEEZ) to calculate the absorbed energy from an array of 200 generic point absorbers.

In chapter II, the methodology of the different steps of the mapping is presented including a description of the wave data set and a description on how energy losses have been included. The results for energy absorption from an array of

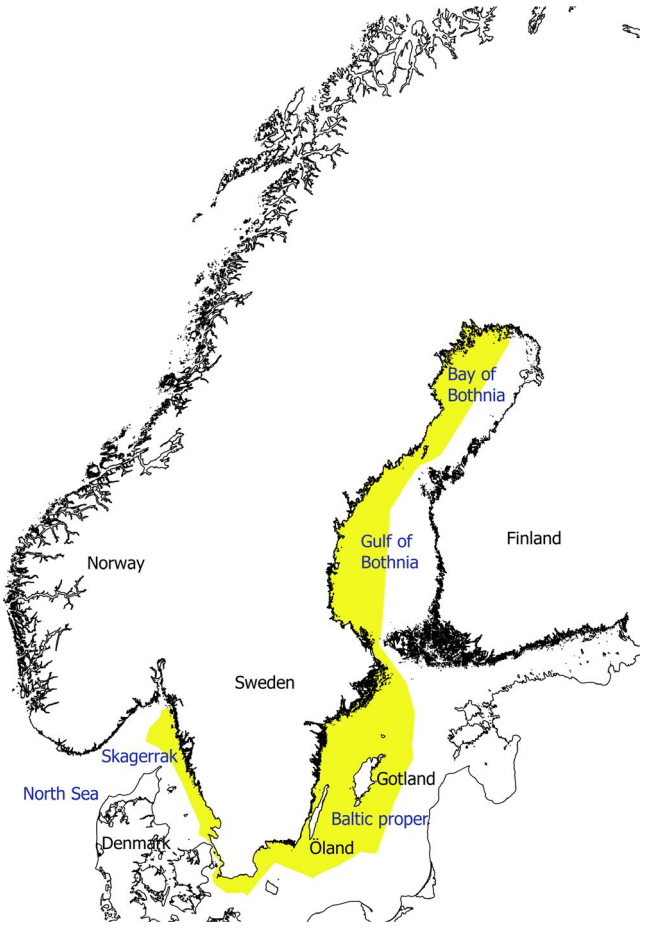

FIGURE 1 Map presenting the sea areas (blue text) discussed in the paper. The yellow area is the Swedish exclusive economic zone

200 WECs both annually and monthly together with energy losses are presented in chapter III. The results and the method are discussed in chapter IV together with some concluding remarks.

2 | METHOD

The Swedish exclusive economic zone, see Figure 1, is divided into a grid with a resolution of 0.01° latitude 0.02° longitude (about 1.1 km) on a spherical grid and the absorbed energy from one park of generic point absorbers in each grid cell are calculated based on the wave climate in each grid cell. In order to do a detailed mapping, some simplifications need to be made for such a complex system as a park of wave energy converters. Further, in this study, we want to have a generic approach and only limit the study to cover wave energy converter of point absorber type.[18] We have chosen to simplify the electric and mechanical parts of the park and have a higher accuracy on the sea states and hydrodynamics. Each WEC is modeled as an ideal mass-damper system consisting of a translator and a semisubmerged cylindrical buoy allowed to move rigidly in heave only. The damping is a linear damping coefficient, implying that the power take off could be electric or hydraulic.

2.1 | Simulation

In each grid cell, several clusters of wave energy converters (WECs) can be deployed and each cluster was chosen to consist of around 50 WECs. In an initial phase of the study, a large number of cluster layouts were studied and the following set up of requirements for the clusters were used as guide lines:

- The cluster (and park) should be as insensitive to wave direction as possible to give generic results on wave energy absorption.
- In all wave directions, there should be as little shadowing effects as possible in order to maximize energy absorption.
- There should be enough space between the WECs to allow for deployment/maintenance and avoid risk for collisions.
- The area should not, however, be too large in order to minimize the cost for sea cable and in order to maximize the number of WECs in a park, since the available ocean area will be restricted.
- The park should have a high power output and low power fluctuations.

Based on these requirements, a star formed cluster of 50 WECs was chosen for the continuation of the project, see Figure 2. Based on this cluster layout, the park layout will consist of 200 WECs located in four clusters, see Figure 2. The locations of the clusters have been chosen to minimize shadowing effects as well as the impact of wave direction.

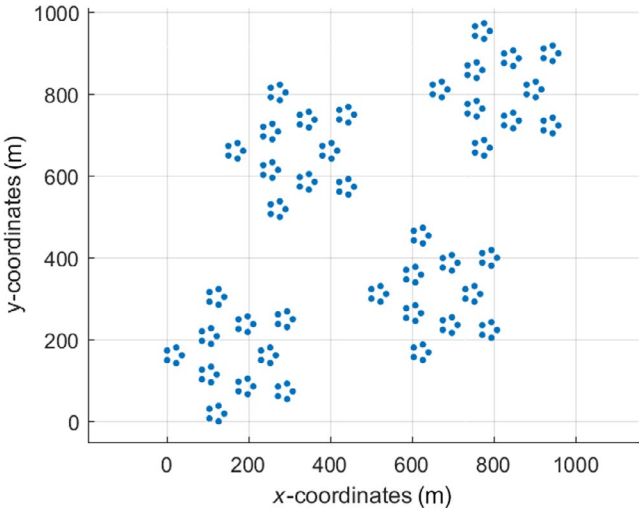

FIGURE 2 Each park consists of four clusters of 50 WECs each, in total 200 WECs

2.1.1 | Hydrodynamic interaction within clusters of 50 WECs

Full hydrodynamic interactions with respect to scattered and radiated waves have been modeled within each cluster consisting of 50 WECs. The modeling is based on linear potential wave theory, which implies an incompressible, nonviscous, and irrotational fluid. Linear theory further implies that the waves have a small amplitude compared with the wave length. This is a simplification and will not be fulfilled for all waves. However, any more detailed method would be impossible to use for large-scale mapping and the WEC model used in this study have been validated with good accuracy against full scale offshore experimental data gathered at the same location as part of the data used in this study.[19] The commercial BEM code WAMIT has been used to model a cluster with 50 WECs with buoy radius $R = 2$ m. However, the computational cost is too high to perform simulations of parks with more WECs or even larger buoy sizes. Therefore, the analytical model of Ref.[20] has been used to model the hydrodynamic interactions in these more computationally costly clusters and parks. The analytical method is based on the theory of multiple scattering; the fluid domain is divided into exterior and interior domains for each buoy, and the solution for the Laplace equation and the linear boundary constraints at the free surface and all rigid boundaries is found by requiring continuity at each domain boundary. After the fluid velocity potential has been determined, the hydrodynamic forces can be obtained as integrals over the wetted surfaces of the

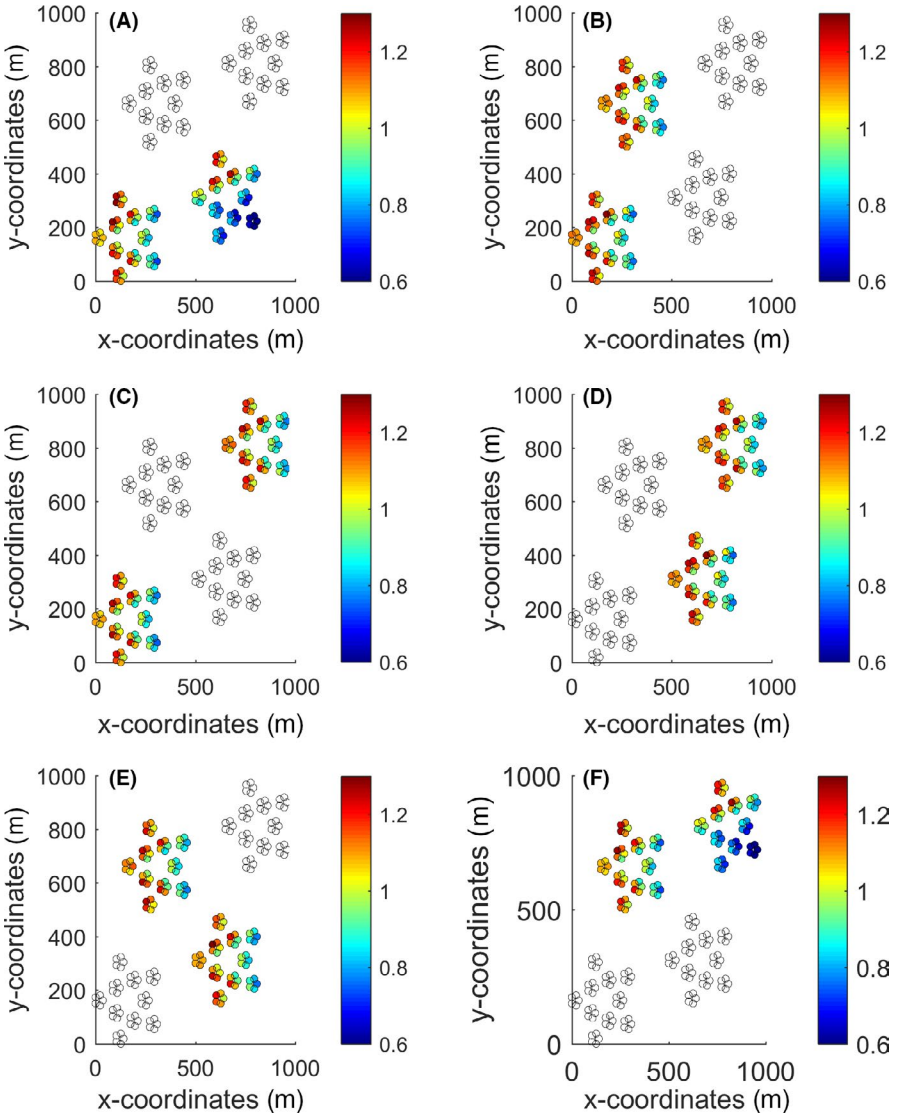

FIGURE 3 Inter-cluster interaction between pairs of clusters in a park. The total park consists of 200 WECs divided into four clusters with 50 WECs in each. The radius of the buoys is $R = 2$ m. In each of the figure, two of the clusters have been coupled hydrodynamically with scattered and radiated waves. The color of each WEC shows the relative energy absorption: The average energy absorption of all WECs is 1; hence, a value above 1 shows that the WEC has an energy absorption above the average in the park. The incident waves are propagating along the x-axis

buoys. The hydrodynamic model has been validated with WAMIT to excellent agreement.[20] A water depth of 50 m has been chosen for all simulations.

2.1.2 | Hydrodynamic interaction within parks of clusters of 200 WECs

With the analytical model, 100 WECs can be modeled with the same accuracy used for a single cluster, that is, exact within the assumptions of linear potential flow theory. A larger number of WECs is, however, not possible to model with the same accuracy and with the available computer resources. Hence, the hydrodynamic interaction within a full park must be modeled by approximate methods. Here, a cluster interaction factor, or q-factor, has been identified for the interaction between each pair of clusters,

$$q_{\text{cluster}} = \frac{[\text{Power from two interacting clusters}]}{[\text{Power from two isolated clusters}]} = \frac{\sum_{i=1}^{100} P_i}{2\sum_{i=1}^{50} P_i}. \quad (1)$$

The results can be seen in Figure 3 and show that, for small buoy radius $R = 2$ m, negative interaction between the clusters occur only when the clusters are directly shadowing each other. In other cases, a slight positive interaction can be detected. However, the hydrodynamic interaction is expected to increase for larger bodies, which will lead to more destructive shadowing effects as will be shown further down. For this simulation, the incident waves are propagating along the x-axis, but due to the symmetry of the park the same results would be obtained if the waves were propagating in the opposite negative x-direction or along the positive or negative y-direction.

In a full park, each cluster will interact with each other cluster in the park, and hence, we compute the total q-factor of the park with N clusters as.

$$q_{\text{park}} = \sum_{j=1}^{n} q_j, n = \binom{N}{2}, \quad (2)$$

where the number of different combinations for $N = 4$ clusters equals $n = 6$. The product of the six q-factors can then be used to compute the total power of the park as.

$$P_{\text{park}} = N q_{\text{park}} P_{\text{cluster}}. \quad (3)$$

In general, the power production will be different in different sea states, which implies that the q-factor will differ between all sea states. Here, an average value of the q-factor in all studied sea states will be used. The computed q-factor for the interaction within a park is shown for the three buoy radii in Table 1. As expected, the destructive interaction increases with increased buoy radius, as the shadowing effect increases. Hence, even though the larger WECs produce more electricity per generator, it is not certain that it will be the most cost-effective solution due to larger capital costs and more destructive interference.

Of the three buoy radii, 2, 3 and 4 m, a buoy with 3 m radius where selected for the mapping since it gave the highest power production.

2.1.3 | Optimal damping and energy absorption

The power production is calculated using the time domain model used in[20] where the power $P(t)$ is obtained as.

$$P(t) = \gamma v(t)^2, \quad (4)$$

where γ is a constant linear damping coefficient that represents the power take off and $v(t)$ is the heave velocity of the buoy. A stiff connection between the surface buoy and the translator is assumed. In the simulations, a total buoy and translator mass of 14 491 kg has been used, which corresponds to a buoy draft of 0.5 m. For all combinations of significant wave height H_s = 0.2:0.2:8 m and peak period T_p = 2:1:16 s, time series of a wave elevation based on the Bretschneider spectrum has been generated and used in the simulations. The two-parameter Bretschneider spectrum is defined as.

$$S_{BS}(\omega) = \frac{1.25}{4}\frac{\omega_p^4}{\omega^5} H_s^2 e^{-1.25(\omega_p/\omega)^2}, \quad (5)$$

where the spectral shape is set by ω_p, which is the peak frequency defined by $\omega_p = 2\pi/T_p$. For each sea state, the optimal damping has been calculated and based on that the averaged power for each WEC is calculated and summarized to give the total power of the park, as shown in Figure 4.

TABLE 1 q-factor for the interaction within a park

Buoy radius	q_{park}
$R = 2$ m	0.9206
$R = 3$ m	0.9080
$R = 4$ m	0.4879

2.2 | Upper theoretical limit

We also calculate a theoretical upper bound for power production based on the buoy volume and the available power in the waves[21]:

$$P_B = \rho g \pi H \pi R^2 h / 4T, \quad (6)$$

$$P_A = \frac{\rho (g/\pi)^3}{128} T^3 H^2, \quad (7)$$

where h is the height of the buoy, which is set equal to the wave height H. The density of sea water is ρ = 1025 kg/m^3, and g = 9.81 m^2/s is the acceleration due to gravity. The upper bounds defined by Equations (6) and (7) are valid for monochromatic waves only, and a conversion from the polychromatic waves is needed to calculate the upper bounds for the energy absorption.

If a monochromatic wave is to have the same energy per surface area as a polychromatic wave it follows that $H = H_s/\sqrt{2}$. And then, it follows that if it is to have the same energy flux as a polychromatic wave $T = T_e$, where T_e is the energy period. Then, an average relation between energy period and the peak period is needed. For all Bretschneider spectra, we have calculated a relation between T_p and T_e to $T_e = 0.856T_p$, which is close to the 0.9 previously used in.[22] Finally, we use the relation that for every sea state the lowest of value of P_B or P_A defines the upper bound. We have included P_B and P_A in order to have a theoretical upper limit to compare to that could be regarded as what a future wave energy converter using some form of optimal control algorithm would absorb in ideal waves.

2.3 | Wave data

A wave hindcast data set of 16 years (1998-2013) of hourly statistics of significant wave height, energy period, peak wave period, and additional parameters was generated based upon wave model results for the Baltic Sea, Skagerrak, and Kattegat area. The WAM Cycle 4 model[23-25] was used with a high horizontal resolution of 0.01° latitude 0.02° longitude (about 1.1 km) on a spherical grid. This is a higher horizontal resolution compared with earlier wave hindcast studies for this area, see[26] for some examples and additional details on the model setup. Seasonal sea ice exists in the Baltic Sea region and was taken into account in the wave modeling by using an ice product based on the operational ice charts produced by the Swedish Ice Service at the Swedish Meteorological and Hydrological Institute (SMHI). If ice concentrations in wet (sea) points were above 30%, they were treated as dry (land)

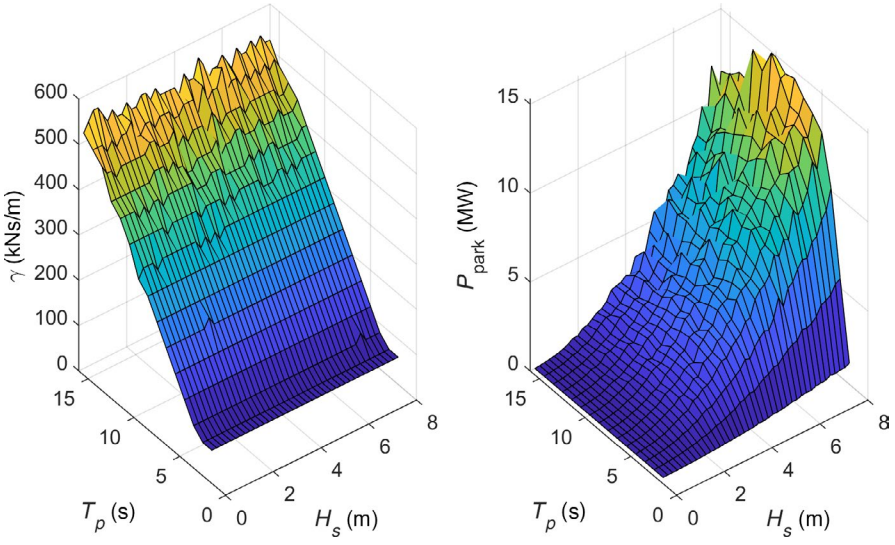

FIGURE 4 Optimal damping γ (left) and the corresponding total power of the park P_{park} (right) in sea states characterized by significant wave height H_s and peak period T_p as given in the figure. The radius of the buoys is $R = 3$ m

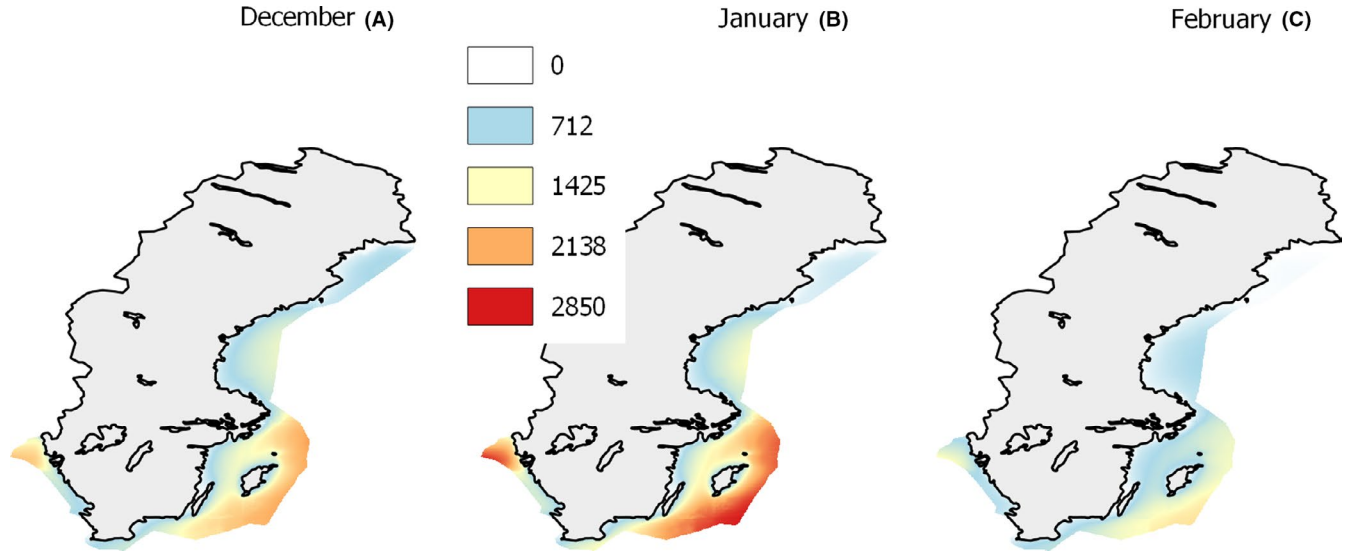

FIGURE 5 A, B C, Average monthly energy absorption E for the winter months December, January, and February. Legends show energy absorption in MWh. The legend is valid for all 3 mo

points for the duration of the ice event similar as in[27] and described further in.[28] The spectral resolution in WAM was set to 24 directions and 35 frequencies, which covers a logarithmically scaled frequency band from 0.042 to 1.07 Hz. The wave hindcast data set is further described in[28] where it is evaluated and theoretical wave energy potential was assessed and some comparison to the Baltic Sea as a whole is presented. The significant wave height for the data set evaluated against 14 wave records from 11 locations in or near the Swedish exclusive economic zone has an overall bias of −0.06 m, average root-mean square error of 0.26 m, and linear correlation coefficient of 0.92 between measurements and model. These error statistics are similar compared with other third-generation wave modeling results[29,30] and indicate in general a good level of agreement between measurements and hindcast results.

2.4 | Mapping

The wave statistics H_s and T_p are sorted into a scatter diagram for each grid cell and each month for all 16 years. The absorbed energy E, see Figure 5, is obtained by multiplying the P_{park} value in each $[H_s, T_p]$ cell in the power matrix with the number of hours in the corresponding $[H_s, T_p]$ cell in the scatter diagram. The theoretical upper bounds P_A and P_B in Equations (7) and (6) are used to calculate the corresponding upper bound for energy absorption E_{ub} in the same manner as E based on all scatter diagrams.

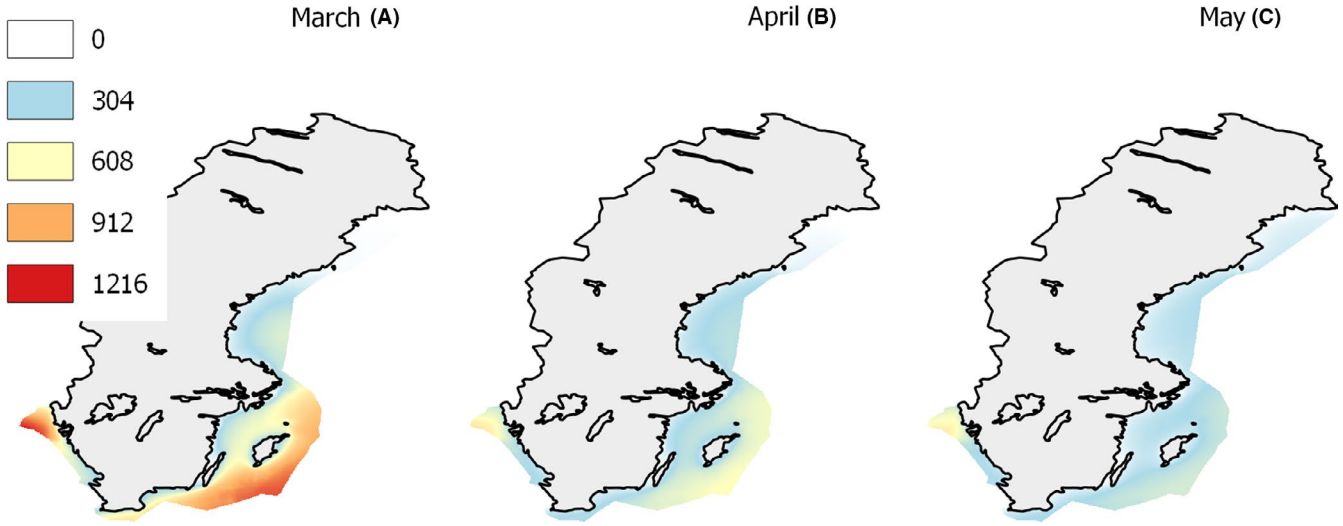

FIGURE 6 A, B, C, Average monthly energy absorption *E* for the spring months March, April, and May. Legends show energy absorption in MWh. The legend is valid for all 3 mo

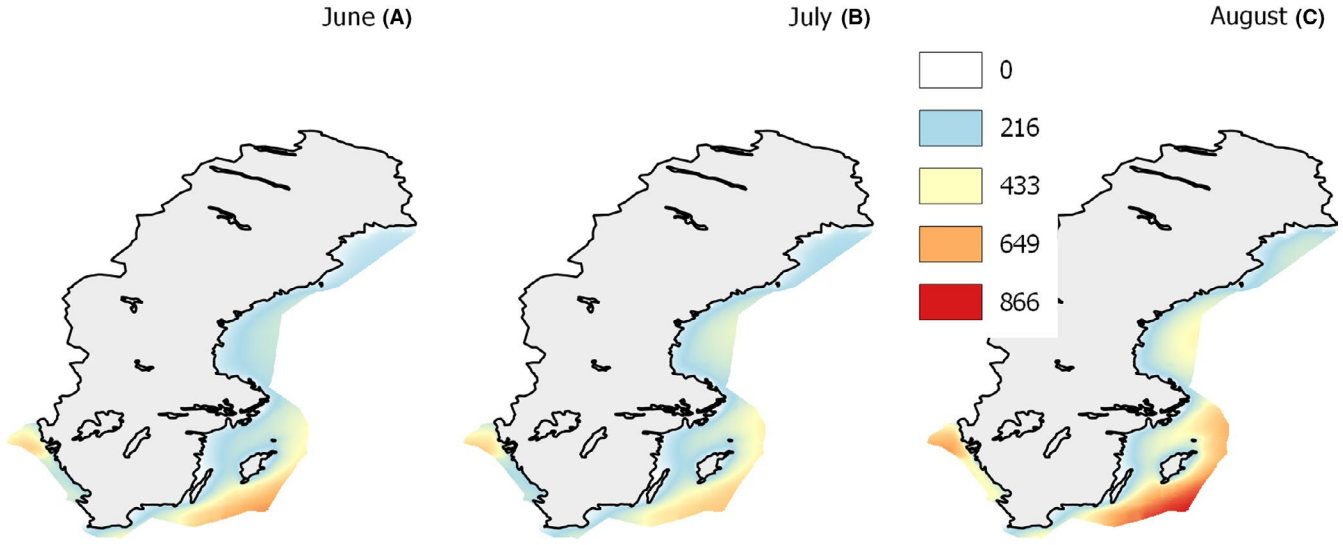

FIGURE 7 A, B, C, Average monthly energy absorption *E* for the summer months June, July, and August. Legends show energy absorption in MWh. The legend is valid for all 3 mo

2.5 | Energy losses

A major factor for any energy converting technology is the energy losses associated with conversion and transmission. In this study, we have excluded losses in the conversion since it inevitably would violate the generic nature of the study. We have, however, included losses in the transmission between the wave energy park and grid, which is especially important in this mapping since each grid cell have a different (and often long) distance to shore which might be a substantial factor on the power production. Since we cannot include information of the load (the grid) in this type of mapping we are restricted to calculate purely resistive losses.

Due to the generic approach we have no specific installed capacity of the wave power park in this study. However, if we assume a capacity of 10-15 MW based on our calculations, we can use that a wind power installation with that capacity normally are connected to a 40 kV medium voltage system. We have therefore chosen a standard 240 mm^2 36 kV transmission cable with a conductor resistance R of 0.125 Ω/km for calculating the transmission losses as:

$$I = \frac{P_{\text{park}}}{3U} \tag{8}$$

$$P_{\text{loss}} = 3I^2RL \tag{9}$$

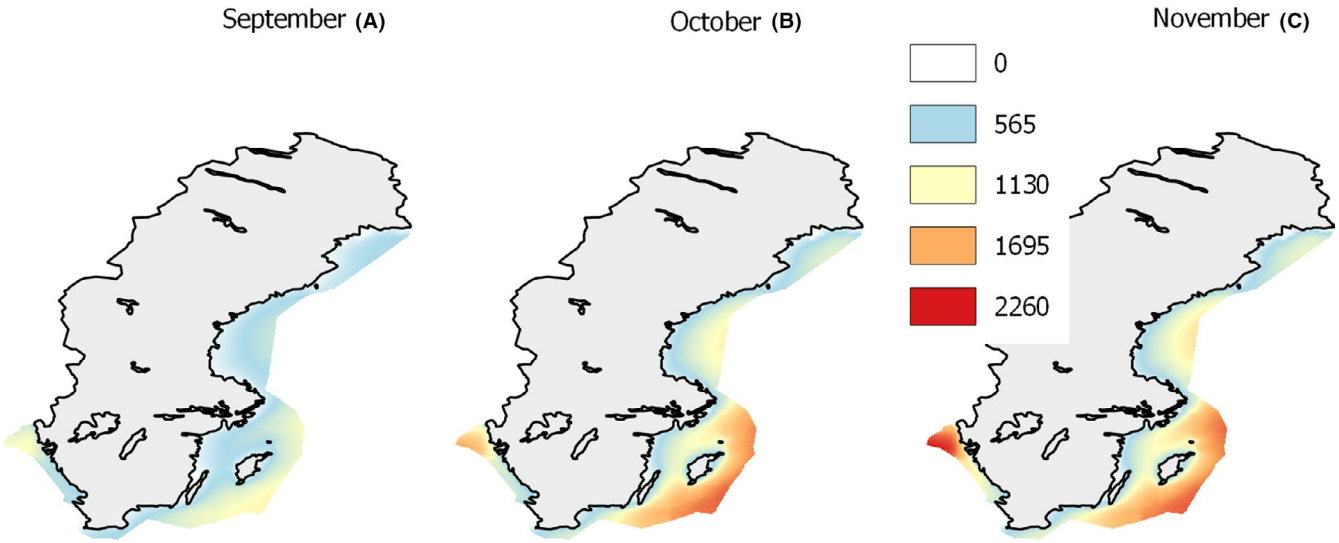

FIGURE 8 A, B, C, Average monthly energy absorption E for the autumn months September, October, and November. Legends show energy absorption in MWh. The legend is valid for all 3 mo

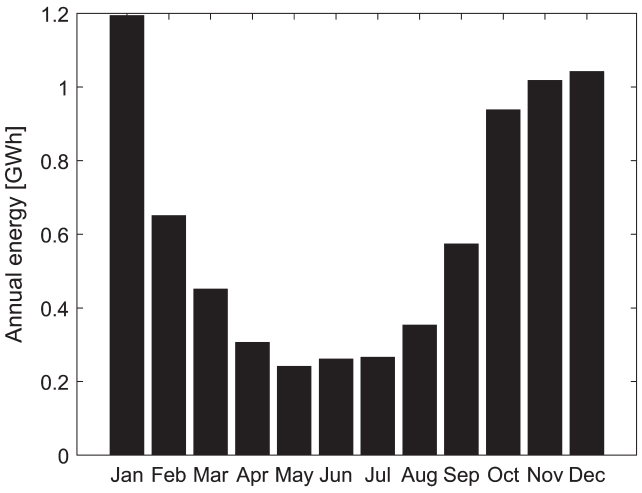

FIGURE 9 Average annual energy absorption E for each month normalized by the number of grid points and number of years

were U and I are the phase voltage and line current and L the distance to shore from the grid cell. The distance to shore L is calculated for each grid cell. P_{loss} are calculated for each $[H_s, T_p]$ cell in the power matrix and multiplied with the corresponding number of hours of the wave energy scatter diagram for each grid cell to give the total average energy losses for each month and each grid cell in exactly the same manner as the energy absorption.

3 | RESULTS

The results in Figures 5-10 are based on all 16 years of wave data. For every month, we have summed the absorbed energy from each year and normalized with the number of years. And by that created an average monthly value based on 16 years, see Figures 5-8. Not surprisingly, the energy absorption follows the seasonal wind patterns of northern Europe with highest values in late autumn and winter and lowest during late spring and summer.

Figure 9 shows the sum of energy absorption of all grid points for all years normalized by the number of grid points and number of years, in order to represent a single value for the energy absorption for the whole area per month. January is the month with highest energy absorption with 1.2 GWh as an average for all grid points, see Figure 9. January is followed by the months December, November, and October, all 3 months have an absorption of around 1 GWh. The lowest value for absorbed energy is found in the period May-July with just above 0.2 GWh.

In Figure 10(A,B) we have summed the absorbed energy from all years and normalized with the number of years and created an annual average for both the case of optimal constant damping as well as for the theoretical upper bound.

In Figure 10(A,B), we can see that the areas with highest absorption are Skagerrak and Baltic proper east of the Islands Öland and Gotland. The areas show an average annual energy absorption of 16 GWh. The absorption calculated based on the theoretical upper bound is constantly around four times higher than the absorption based on the optimal constant damping case.

Power losses depend on both the power level and the length of the cable. Therefore, the areas with highest energy absorptions northeast and southeast of Gotland and northern Skagerrak have the highest energy losses of up to 4.5% of absorbed energy with this cable as can be seen in Figure 11. But the losses dependence on distance to shore gives that also

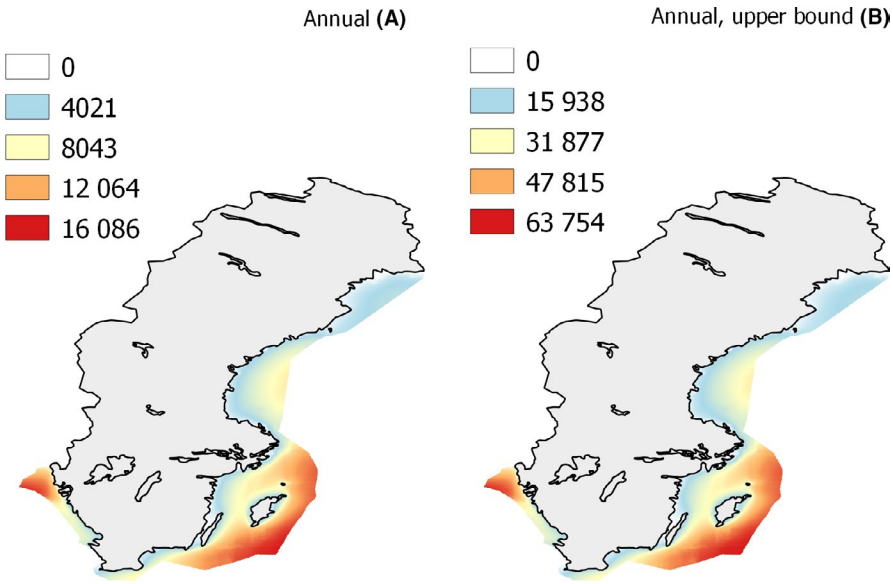

FIGURE 10 A, B, Average annual energy absorption E in (A) and (B) shows the average annual energy absorption based on the upper bound E_{ub}. Legends show energy absorption in MWh

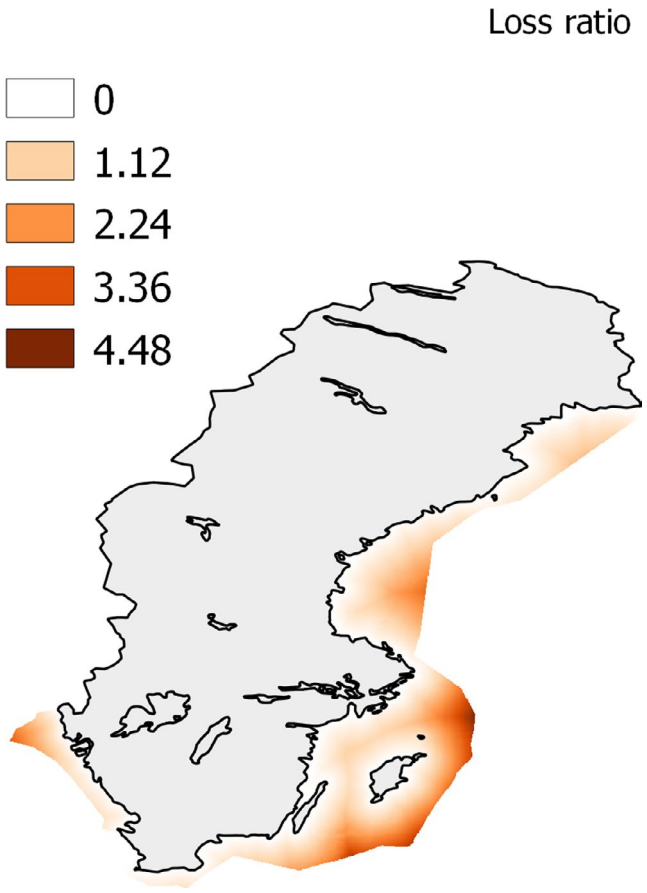

FIGURE 11 Average annual energy losses in percent of absorbed energy for a 240 mm^2 36 kV transmission cable between the wave energy park and shore

a narrow band between Gotland and main land as well as the central Gulf of Bothnia shows higher losses. Thus, the latter are areas with both low absorption levels as well as higher losses.

4 | DISCUSSION AND CONCLUSIONS

The energy absorption in February Figure 5(C) is lower than shown in[9] where February was identified as the month with the highest energy flux at the Swedish west coast. The study in[9] is based on 8 years of wave data (1997-2004) calibrated at one site by a wave measurement buoy. This difference is partly explained by the presence of sea ice in the Gulf of Bothnia and the Bay of Bothnia. Maximum sea ice extent in the area is normally in February and March.[31] The very low values for energy absorption in especially Bay of Bothnia in February and March are visible in Figures 5(C) and 6(A). But we can also see that the values for the Swedish west coast and the Baltic proper are lower in February then in January and December and this cannot be explained by the presence of sea ice since it is an area that are normally ice free. However, Ref.[30] shows that for the studied period (1965-2005) the highest average wind speed was in January and that 84% of the of the sea states with a significant wave height above 7 m was during November-January. This study is partly in line with Figure 9 but excludes the Swedish west coast. In an early wave model study from 2003 for 1 year of simulation (1999) at about 11 km horizontal resolution,[10] December and November were found to be the months with highest significant wave height, not January.

The high values for energy absorption in January in this study could be explained by a combination of easterly and westerly storms that are common in the winter. Since the values for energy absorption in Figure 9 are a sum for the whole area, it will receive input for both easterly and westerly storms. The contribution from easterly storms for the energy flux at the west coast in[9] is almost zero due

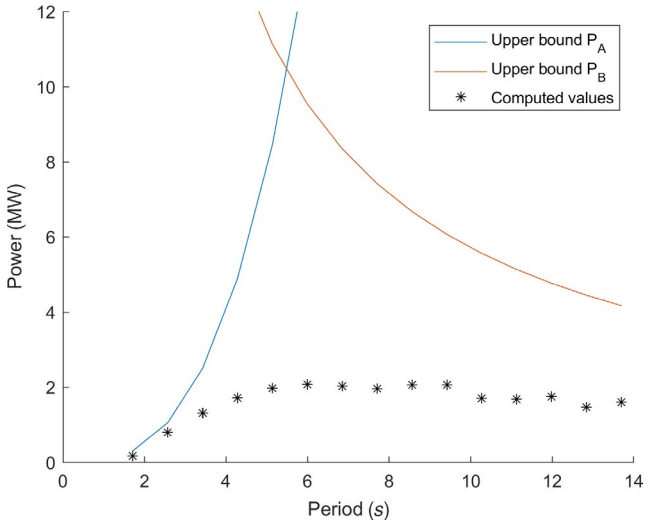

FIGURE 12 The theoretical upper bound for power production based on the buoys volume P_B and the available power in the waves P_A. The line marked by stars is the computed values of P_{park} for optimal constant damping and for a significant wave height H_s of 1.6 m

to the small fetch. This points out the interesting fact that countries with coasts facing both to the east and west like Sweden will get a lower annual intermittency in the power production from wave energy since it benefits from both westerly and easterly storms. The predominant wind direction at these latitudes are, however, from southwest and westerly or southwesterly wave directions are therefore more frequent for this region.

It should be noted that the comparison to previous wave climate studies made here are only indicative since they do not cover the same time periods and maximum significant wave height do not directly correspond to high annual energy absorption for a wave energy park.

Skagerrak at the Swedish west coast are normally regarded as the area with best potential for wave energy in Sweden since it faces the North Sea. However, we can see in Figure 10 that the southern tip of Öland and Gotland are equally interesting areas. Or, maybe even more interesting since it receives waves from all directions except north and northeast leading to a lower annual intermittency compared with Skagerrak.

With a layout of WECs based on the requirements stated in Section 2.1, the areas with the best technical potential have an average annual energy absorption of 16 GWh with the optimal constant damping and 63 GWh for the theoretical upper bound. However, the WEC layout only occupies about 0.84 km^2, see Figure 2, resulting in an adjusted absorbed energy per square kilometer of 19 GWh/km^2 for the optimal constant damping and 75 GWh/km^2 for the theoretical upper bound.

The generic approach to wave energy conversion in this paper does not specify a WEC technology well enough to allow any form of cost comparison with alternative technologies. However, a simple comparison of absorbed energy per square kilometer could be made. It may be interesting to compare the simulated wave power plant to a large solar power plant and an offshore wind power farm in the same region. Varberg Energi's *Solsidan* solar power plant at the Swedish west coast with a capacity of 2.7 MW covers an area of 0.06 km^2. *Solsidan* solar power plant has an annual electricity generation of 3 GWh,[32] or 50 GWh/km^2 which gives a capacity factor of 12.3%. Vattenfall's *Lillgrund* offshore wind power farm is located in Öresund, between Sweden and Denmark. *Lillgrund* wind power farm covers an area of around 8 km^2 and has a capacity of 110 MW *Lillgrund* produces around 330 GWh annually,[33] which gives a capacity factor of 34% and an electricity generation of 41 GWh/km^2. In this comparison, solar power produces 2.5 times more and wind power 2 times more than the simulated wave power of 19 GWh/km^2 with constant damping. But firstly, the Swedish wave climate is very mild. The nearby European Atlantic coasts have an energy flux more than 10 times higher.[1] Secondly, the optimal constant damping is a conservative approach. The simulated theoretical upper bound of 75 Gwh/km^2 is on the other hand 1.5 times higher than solar power and 1.8 times higher than wind power, per square kilometer. In Figure 12, we have plotted the theoretical upper bound for power production based on the buoys volume P_B (Equation 6) and the available power in the waves P_A (Equation 7) and compared with the computed values of P_{Park} (Equation 3) for optimal constant damping.

With the constant damping approach, the WEC has a high power capture compared with P_A for the very smallest waves. But when approaching the most common sea states with a wave period of 5-6 seconds the power capture decreases to 30% and lower of what is available in the wave, see Figure 12. It has been shown theoretically that adaptive control methods like complex conjugate control, model predictive control, and latching absorb far more energy than passive control and approaches the theoretical bounds.[34] Thirdly, a comparison based on annual energy converted per square kilometer it is not a valid argument for investment purposes. Comparisons are not performed on the basis of the area that the technology occupies, even though land may have a substantial cost attached to it, as in the case for solar power plants and onshore wind power farms. Instead, comparisons are made from the standpoint of a selected technology with known and established cost levels. With a generic approach to a noncommercialized and relatively immature technology, such as wave power, a comparison is not yet possible.

Compared with a solar power plant, the wave energy converters (WECs) cover just a small fraction of the occupied area since WECs are relatively small. This means that the direct environmental effects are small, and most of the occupied area can be used by other interests. A solar power plant covers more or less the whole occupied area unless it is integrated in buildings. On the other hand, we have excluded all electrical and mechanical energy losses inside the WECs and at the site, which of course will reduce the electricity generation. As clarified in the paper, unavoidable simplifications are made on the electrical, mechanical, and hydrodynamic parts of the simulation, partly to maintain the generic approach to WEC design. In other words, this is just an estimation, which most probably overestimates the energy absorption to some extent. Also, with our approach, the wave energy park will produce power for all sea states. This is a rather generous approach. The electric system for a future commercial wave energy park will most probably be dimensioned for the most common sea state and somehow be ramped down in higher sea states, just like a wind power farm.

Comparing different electric power generating technologies is not straightforward.[35-38] It involves a lot of aspects, which can be valued differently. A high capacity factor, for instance, could in theory increase the statistical probability of providing electricity during times of peak demand, which may vary from site to site and region to region for intermittent renewable energy. The price of electricity varies with demand and lower market prices results in lower revenues for producers. Surplus power production during times of off-peak demand have even led to negative prices in certain European countries, that is, Germany,[39,40]. A substantial investment in equipment for energy storage, such as large battery installations, aims to solve problems with intermittency to enable a comparison between intermittent renewable and dispatchable energy technologies. However, for investments in photovoltaics (PV), the cost for equipment related to energy storage has been quantified to almost three times the investment cost of the actual power generating technology itself in $/MWh[41], but the costs will decrease over time. If wave power would mature to the current level of wind and solar, it would probably be less dependent on energy storage due to a higher capacity factor and thereby offer an increased ability to provide electricity during times of peak demand and thereby benefit from high market prices.

In order for wave power to develop, park size power plants need to be established at suitable pilot sites to demonstrate park size plant performance in the coming years. The Swedish wave energy resource mapping (SWERM) project,[26,28] a national project conducted by Uppsala University and partners from which this paper is produced, aims to facilitate the potential introduction of wave power in the best locations within the SEEZ. The technical potential estimated through the presented simulations will be used along with other relevant mapped variables studied in the SWERM project to locate the most promising locations with a 1 km^2 grid resolution.

ACKNOWLEDGMENT

The authors would like to thank The Swedish Energy Agency for funding this project (Project no. 42256-1) within the national Swedish research program for marine energy conversion. The Swedish STandUP for Energy research alliance, a collaboration initiative financed by the Swedish government, is acknowledged for contributing to the research infrastructure.

ORCID

Jens Engström https://orcid.org/0000-0002-2031-8134

REFERENCES

1. Mørk G, Barstow S, Kabuth A, Pontes MT. Assessing the Global Wave Energy Potential. In: *29th International Conference on Ocean, Offshore and Arctic Engineering*. Vol. 3. Shanghai, China: American Society of Mechanical Engineers; 2010:447-454.
2. Pontes MT. Assessing the European wave energy resource. *J Offshore Mech Arct Eng*. 1998;120(4):226.
3. Henfridsson U, Neimane V, Strand K, et al. Wave energy potential in the Baltic Sea and the Danish part of the North Sea, with reflections on the Skagerrak. *Renew Energy*. 2007;32(12):2069-2084.
4. Bernhoff H, Sjöstedt E, Leijon M. Wave energy resources in sheltered sea areas: a case study of the Baltic Sea. *Renew Energy*. 2006;31(13):2164-2170.
5. Sorensen HC, Fernandez Chozas J. The Potential for Wave Energy in the North Sea. Presented at the International Conference on Ocean Energy, Bilbao, Spain, 2010.
6. Kim C-K, Toft JE, Papenfus M, et al. Catching the right wave: evaluating wave energy resources and potential compatibility with existing marine and coastal uses. *PLoS ONE*. 2012;7(11):e47598.
7. Yemm R, Pizer D, Retzler C, Henderson R. Pelamis: experience from concept to connection. *Philos Trans A Math Phys Eng Sci*. 2012;370(1959):365-380.
8. Iglesias G, López M, Carballo R, Castro A, Fraguela JA, Frigaard P. Wave energy potential in Galicia (NW Spain). *Renew Energy*. 2009;34(11):2323-2333.
9. Waters R, Engström J, Isberg J, Leijon M. Wave climate off the Swedish west coast. *Renew Energy*. 2009;34(6):1600-1606.
10. Jönsson A, Broman B, Rahm L. Variations in the Baltic Sea wave fields. *Ocean Eng*. 2003;30(1):107-126.
11. Falnes J. Wave-power absorption by an array of attenuators oscillating with unconstrained amplitudes. *Appl Ocean Res*. 1984;6(1):16-22.
12. Simon MJ. Multiple scattering in arrays of axisymmetric wave-energy devices. Part 1. A matrix method using a plane-wave approximation. *J Fluid Mech*. 1982;120(1):1.
13. Engström J, Eriksson M, Göteman M, Isberg J, Leijon M. Performance of large arrays of point absorbing direct-driven wave energy converters. *J Appl Phys*. 2013;114(20):204502.

14. Göteman M, Engström J, Eriksson M, Isberg J. Optimizing wave energy parks with over 1000 interacting point-absorbers using an approximate analytical method. *Int J Marine Energy*. 2015;10:113-126.
15. Blavette A, O'Sullivan DL, Lewis AW, Egan MG. Impact of a wave farm on its local grid: Voltage limits, flicker level and power fluctuations. In 2012 Oceans - Yeosu, Yeosu, Korea (South), 2012:1-9.
16. Kavanagh D, Keane A, Flynn D. Challenges posed by the integration of wave power onto the Irish power system. presented at the European Wave and Tidal Energy Conference, Southampton, UK, 2011.
17. Ekström R, Leijon M. Control of offshore marine substation for grid-connection of a wave power farm. *Int J Marine Energy*. 2014;5:24-37.
18. Budar K, Falnes J. A resonant point absorber of ocean-wave power. *Nature*. 1975;256(5517):478-479.
19. Eriksson M, Waters R, Svensson O, Isberg J, Leijon M. Wave power absorption: experiments in open sea and simulation. *J Appl Phys*. 2007;102(8):084910.
20. Göteman M, Engström J, Eriksson M, Isberg J. Fast modeling of large wave energy farms using interaction distance cut-off. *Energies*. 2015;8(12):13741-13757.
21. Falnes J. *Ocean Waves and Oscillating Systems: Linear Interactions Including Wave-Energy Extraction*. Cambridge: Cambridge University Press; 2002.
22. Pastor J, Liu Y. Retracted: "Wave Energy Resource Analysis for Use in Wave Energy Conversion" [ASME Journal of Offshore Mechanics and Arctic Engineering, 137 (1), p. 011903]. *J Offshore Mech Arctic Eng*. 2014;137(1):011903.
23. T. W. Group. The WAM model—A third generation ocean wave prediction model. *J Phys Oceanogr*. 1988;18(12):1775-1810.
24. Günther H, Hasselmann S, Janssen PAEM. The WAM Model cycle 4. 2009.
25. Komen GJ, Cavaleri L, Donelan M, Hasselmann K, Hasselmann S, Janssen P. *Dynamics and Modelling of Ocean Waves*. Cambridge: Cambridge University Press; 1994.
26. Strömstedt E, Haikonen K, Engström J, et al. On defining wave energy pilot sites in Swedish Seawaters. presented at the 12th European wave and tidal energy conference, Cork, Ireland, 2017.
27. Tuomi L, Kahma K, Pettersson H. Wave hindcast statistics in the seasonally ice-covered Baltic Sea. *Boreal Environ Res*. 2011;16:451-472.
28. Nilsson E, Rutgersson A, Dingwell A, et al. Characterization of wave energy potential for the Baltic sea with focus on the Swedish exclusive economic zone. *Energies*. 2019;12(5):793.
29. Iuppa C, Cavallaro L, Vicinanza D, Foti E. Investigation of suitable sites for Wave Energy Converters around Sicily (Italy). *Ocean Sci Discussions*. 2015;12(1):315-354.
30. Björkqvist J-V, Lukas I, Alari V, et al. Comparing a 41-year model hindcast with decades of wave measurements from the Baltic Sea. *Ocean Eng*. 2018;152:57-71.
31. Löptien U, Dietze H. Sea ice in the Baltic Sea–revisiting BASIS ice, a historical data set covering the period 1960/1961–1978/1979. *Earth System Science Data*. 2014;6(2):367-374.
32. Varberg Energi. http://www.varbergenergi.se/om-oss/var-verksamhet/sol/solsidan/. Accepted February 12, 2019.
33. Vattenfall. https://corporate.vattenfall.se/om-oss/var-verksamhet/var-elproduktion/vindkraft/lillgrund-vindkraftpark/. Accepted June 09, 2016.
34. Hals J, Falnes J, Moan T. A comparison of selected strategies for adaptive control of wave energy converters. *J Offshore Mech Arct Eng*. 2011;133(3):031101.
35. Larsson S, Fantazzini D, Davidsson S, Kullander S, Höök M. Reviewing electricity production cost assessments. *Renewable and Sustainable Energy Reviews*. 2014;30:170–183.
36. Joskow PL. Comparing the Costs of Intermittent and Dispatchable Electricity Generating Technologies. *American Economic Review*. 2011;101(3):238–241.
37. Hansen K. Decision-making based on energy costs: Comparing levelized cost of energy and energy system costs. *Energy Strategy Reviews*. 2019;24:68–82.
38. Ueckerdt F, Hirth L, Luderer G, Edenhofer O. System LCOE: What are the costs of variable renewables? *Energy*. 2013;63:61–75.
39. Nicolosi M. Wind power integration and power system flexibility–An empirical analysis of extreme events in Germany under the new negative price regime. *Energy Pol*. 2010;38(11):7257-7268.
40. Valitov N. Risk premia in the German day-ahead electricity market revisited: the impact of negative prices. *Energy Econ*. 2018:1-7.
41. Baum S, von Kalben C, Maas A, Stadler I. Analysis and Modelling of the Future Electricity Price Development by taking the Levelized Cost of Electricity and large Battery Storages into Account. In: 2018 7th International Energy and Sustainability Conference (IESC), Cologne, Germany, 2018:1-8.

How to cite this article: Engström J, Göteman M, Eriksson M, et al. Energy absorption from parks of point-absorbing wave energy converters in the Swedish exclusive economic zone. *Energy Sci Eng*. 2019;00:1–12. https://doi.org/10.1002/ese3.507